Research Article | Vol. 28, No. 24 / 23 November 2020 / Optics Express 36466
Optics EXPRESS

Kicking the habit/semiconductor lasers without isolators

MARK HARFOUCHE,[1,5,*] DONGWAN KIM,[2,5] HUOLEI WANG,[2,5] CHRISTOS T. SANTIS,[2] ZHEWEI ZHANG,[2] HETUO CHEN,[2,3] NARESH SATYAN,[4] GEORGE RAKULJIC,[4] AND AMNON YARIV[1,2]

[1]*Department of Electrical Engineering, California Institute of Technology, 1200 E. California Blvd., Pasadena, CA 91125, USA*
[2]*Department of Applied Physics and Materials Science, California Institute of Technology, 1200 E. California Blvd., Pasadena, CA 91125, USA*
[3]*Shanghai Institute of Ceramics, Chinese Academy of Sciences, Shanghai, 200050, China*
[4]*Telaris Inc., 2118 Wilshire Blvd., Santa Monica, CA 90403, USA*
[5]*These authors all equally contributed to the work*
[*]*mark.harfouche@caltech.edu*

Abstract: In this paper, we propose and demonstrate a solution to the problem of coherence degradation and collapse caused by the back reflection of laser power into the laser resonator. The problem is most onerous in semiconductor lasers (SCLs), which are normally coupled to optical fibers, and results in the fact that practically every commercial SCL has appended to it a Faraday-effect isolator that blocks most of the reflected optical power preventing it from entering the laser resonator. The isolator assembly is many times greater in volume and cost than the SCL itself. This problem has resisted a practical and economic solution despite decades of effort and remains the main obstacle to the emergence of a CMOS-compatible photonic integrated circuit technology. A simple solution to the problem is thus of major economic and technological importance. We propose a strategy aimed at weaning semiconductor lasers from their dependence on external isolators. Lasers with large internal Q-factors can tolerate large reflections, limited only by the achievable Q values, without coherence collapse. A laser design is demonstrated on the heterogeneous Si/III-V platform that can withstand 25 dB higher reflected power compared to commercial DFB lasers. Larger values of internal Qs, achievable by employing resonator material of lower losses and improved optical design, should further increase the isolation margin and thus obviate the need for isolators altogether.

1. Introduction

We propose and demonstrate theoretically and experimentally a simple yet fundamental solution to the problem of feedback sensitivity in semiconductor lasers. It is realized by employing laser resonators with very large values of internal Q-factor. Such resonators have become possible with the advent of the Silicon (Si) photonics platform [1,2] and employ a new laser resonator design wherein the majority of the optical energy resides not in the active region, which is the legacy design [3–5], but in a new low-loss Si guiding layer, which is an intrinsic part of the laser waveguide, up to ~ 99% in our case [6,7]. This reduces the power dissipated within the resonator by close to two orders of magnitude.

This extreme loss reduction enables the use of output-side laser reflectivity approaching unity without, surprisingly at first, sacrificing output power. This is due to the orders of magnitude increase in the internal stored optical energy attendant on the high-Q resonator design which compensates, under the right conditions, described in what follows, for the reduced output coupling.

#411816 https://doi.org/10.1364/OE.411816
Journal © 2020 Received 6 Oct 2020; revised 6 Nov 2020; accepted 7 Nov 2020; published 16 Nov 2020

Optics EXPRESS

These high values of output reflectivity, in turn, allow only a minute fraction, <1% in our demonstration, of the reflected power from entering the laser resonator and degrading its coherence. Such lasers *do not* require optical isolators. While the demonstration is done on a heterogeneous Si/III-V platform, the reported findings are independent of the choice of gain material making the findings of extreme importance to all integrated laser design.

This paper is organized as follows: following the basic laser theory background, we describe the design details of the high-Q heterogeneous Si/III-V laser used in our demonstration. Second, we briefly discuss the particular laser structure and fabrication techniques used in the demonstration. Finally, we share the results from the experiments used to characterize the onset of coherence collapse in our lasers.

2. Engineering the feedback sensitivity of semiconductor lasers

Most treatments of the effect of feedback on the laser field coherence start with the model and analysis of Petermann [8–10]. The laser and external feedback are illustrated in Fig. 1. The laser output mirror reflectance is denoted with r_{2s}, while the feedback of magnitude is characterized by a reflectance of r_{2ext} at a distance L_{ext} away from the facet of the laser. The effect of the feedback on the laser oscillation can be accounted for, provided that $|r_{2ext}| \ll |r_{2s}|$, by replacing the reflectance r_{2s} by a complex reflectance given by

$$r_{eff} = r_{2s} + r_{2ext}\left(1 - |r_{2s}|^2\right) e^{-i2\pi\nu\tau_{ext}}. \tag{1}$$

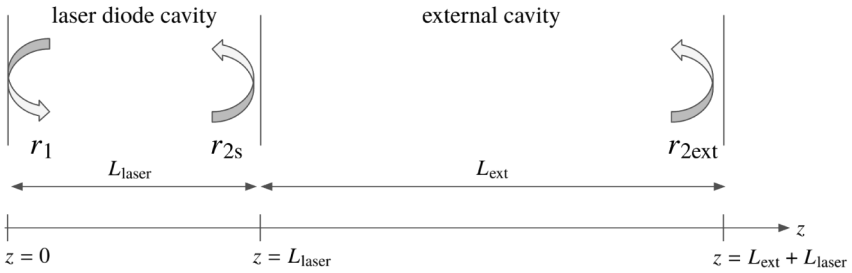

Fig. 1. The Petermann model for a laser resonator with an external, undesired reflector.

The frequency dependence of the complex r_{eff} modifies the longitudinal unperturbed resonant frequencies of the Fabry-Perot resonator such that, above a certain level of feedback, multi-mode oscillation becomes possible. This multimode oscillation is the death knell for the laser field coherence. The onset of multimode oscillation occurs when the following Petermann parameter (C) exceeds unity [8],

$$C = \frac{\tau_{ext}}{\tau_{laser}} \frac{r_{2ext}}{r_{2s}} \left(1 - |r_{2s}|^2\right) \sqrt{1 + \alpha^2}, \tag{2}$$

where $\tau_{laser} \equiv \frac{2n_{laser}L_{laser}}{c}$, $\tau_{ext} \equiv \frac{2nL_{ext}}{c}$, and n_{laser} and n are the effective indices of refraction of the laser waveguide and output fiber, respectively. α is the phase-amplitude coupling parameter of the laser medium (the Henry parameter) [11,12]. c is the velocity of light in vacuum.

A concern of the analysis above is that while C depends on two laser parameters, α and r_{2s}, it also depends on τ_{ext}, a parameter of the uncontrolled external reflector. For reflectors very far away from the laser, τ_{ext} can be so large that it can cause mode-hopping even for extremely small values of r_{2ext} before eventually causing coherence collapse for larger external reflectors. This regime has been analyzed analytically and experimentally in [13–15] to find a closed-form equation for the onset coherence collapse in the regime of large τ_{ext}. Briefly, the insights from [14] can be summarized to show that for reflectors far away from the laser, $2\pi f_r \tau_{ext} \gg 1$, which

Optics EXPRESS

is of critical importance for fiber communication systems, the onset of coherence collapse is no longer dependent on τ_{ext} but only on the laser parameters including α, r_{2s}, the relaxation resonance frequency of the laser f_r, and the damping frequency f_d of the direct modulation response. The laser is considered to reach the coherence collapse regime when:

$$\frac{f_d}{\pi f_r^2}\frac{1}{\tau_{\text{laser}}}\frac{\left|r_{2\text{ext, coherence collapse}}\right|}{|r_{2s}|}\left(1-|r_{2s}|^2\right)\sqrt{1+\alpha^2}>1. \tag{3}$$

A consideration of Eqs. (2) and (3) points directly to two main approaches potentially capable of satisfying the stability condition $C<1$. The first is to choose a semiconductor gain medium such that α, which is a material property, is as small as possible. One such medium is that based on quantum dots (QDs), in which limited improvements in lasers based on QDs have been reported [16–19]. In addition, QDs still remain difficult to grow for certain materials and wavelengths. For lasers systems where QDs are not viable, quantum wells (QWs) often remain as the only option. For QWs, the typical values of α in commercial lasers are in the range of 4-5, such that the expected improvement is not sufficient to obviate the need for external isolators.

The second approach to satisfy the stability condition $C<1$ is, according to Eq. (2), to allow $|r_{2s}|^2$ to approach unity. This is a simple optical solution and is limited only by the ability to achieve high values of reflectivity ($|r_{2s}|^2 \rightarrow 1$). A natural concern of this strategy would be that although we satisfy $C<1$, in this manner the power output, given by,

$$P_{\text{out}} = P_{\text{circulating}}\left(1-|r_{2s}|^2\right), \tag{4}$$

where $P_{\text{circulating}}$ is the internal power incident on the output reflector, will tend to zero. This issue will be addressed next, where it will be shown that for well-designed resonators, the internal circulating power (photon density) can be designed to increase to allow $|r_{2s}|^2$ to approach unity, thus compensating for the reduced transmissivity. Following this strategy, we can, in principle, ensure that a majority of the power emitted by the inverted gain medium becomes available as useful optical output from the laser. The problem becomes essentially that of power output and optimum coupling in laser oscillators [20] and will be considered next.

The total power emitted by stimulated emission in an SCL above the threshold current is [21]

$$P_{\text{stimulated emission}} = \eta\frac{I-I_{\text{th}}}{q}h\nu, \tag{5}$$

where η is the injection quantum efficiency, I is the injection current, I_{th} is the threshold current, q is the electron charge, h is the Planck's constant, and ν is the optical frequency of radiation, approximately 193 THz for the case of 1550 nm lasers. Equation (5) follows from the basic laser theory and is a simple statement of the fact that due to gain clamping, above the current threshold each electron injected into the active region results in one photon emitted into the laser mode. It is convenient to use in the analysis which follows the conventional definition of the resonator Q-factors,

$$Q_{\text{int}} = 2\pi\nu\frac{\text{Energy stored in resonator}}{\text{Power lost within resonator}}, \tag{6}$$

$$Q_{\text{ext}} = 2\pi\nu\frac{\text{Energy stored in resonator}}{\text{Power exiting as output}} = \frac{2\pi\nu\tau_{\text{laser}}}{1-|r_{2s}|^2}. \tag{7}$$

The useful power output of the laser is thus related to the total stimulated emission (Eq. (5)) by the ratio of the external losses (Q_{ext}^{-1}) to the total losses ($Q_{\text{int}}^{-1}+Q_{\text{ext}}^{-1}$),

$$P_{\text{out}} = \eta\frac{I-I_{\text{th}}}{q}h\nu\frac{Q_{\text{ext}}^{-1}}{Q_{\text{ext}}^{-1}+Q_{\text{int}}^{-1}} = \eta\frac{I-I_{\text{th}}}{q}h\nu\frac{1}{1+\frac{Q_{\text{ext}}}{Q_{\text{int}}}} = \eta\frac{I-I_{\text{th}}}{q}h\nu\frac{1}{1+\frac{2\pi\nu\tau_{\text{laser}}}{Q_{\text{int}}\left(1-|r_{2s}|^2\right)}}. \tag{8}$$

Equation (2) tells us what values of output reflectivity $|r_{2s}|^2$ are needed in a given scenario to satisfy the stability condition $C<1$ and thus achieve feedback insensitivity, while Eq. (8)

Optics EXPRESS

determines the emitted useful power for a given $|r_{2s}|^2$. We have neglected the small dependence of I_{th} on Q_{int} near $Q_{int} \approx Q_{ext}$. This has been checked in numerical simulations [22].

Equation (8) also shows that increasing the reflectivity of the output mirror can be used to increase the optical isolation without sacrificing the output power so long as $Q_{ext} \ll Q_{int}$. If we

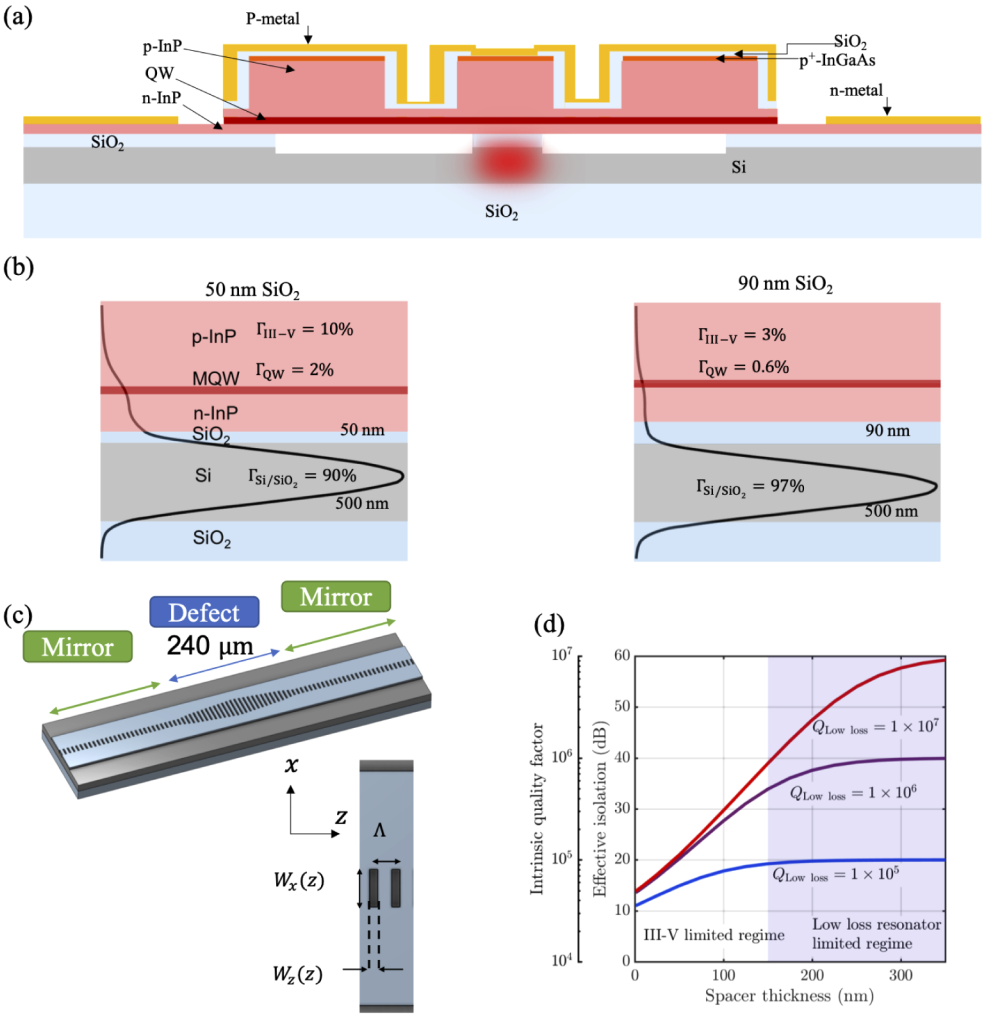

Fig. 2. (a) The depiction of the cross-section of the high-Q heterogeneous Si/III-V laser structure showing the location of the optical mode, III-V mesa, and electrical contacts used to pump the laser. (b) The detailed cross-section of the laser structure showing the intensity of the optical mode for the case of the 50 nm (left) and the 90 nm spacer (right) with $\Gamma_{III\text{-}V} = 10\%$ and $\Gamma_{III\text{-}V} = 3\%$, respectively. (c) The cartoon of the Si resonator structure showing the defect section and the mirror sections. The inset shows two unit cells of the grating and labels the relevant dimensions of the 1D photonic crystal used to engineer the photonic bandgap in the laser cavity. (d) The effective increase in the intrinsic Q-factor of the laser and its optical isolation as the thickness of the SiO_2 spacer layer is increased. The shaded area shows the region where the Q-factor of the resonator is limited by that of the low-loss material for the case of our Si resonator where the Q_{int} is estimated to be on the order of 1×10^6. If the Q-factor of the low loss material is increased to 1×10^7, an effective optical isolation of more than 50 dB is achievable.

Optics EXPRESS

are willing to settle for a compromise between maximum optical isolation and good optical power efficiency, let that be 50% power efficiency, i.e., $P_{\text{out}}/P_{\text{stimulated emission}} \geq 0.5$, we can derive the following inequality from Eqs. (5) and (8),

$$Q_{\text{int}} \geq \frac{2\pi\nu\tau_{\text{laser}}}{\left(1-|r_{2s}|^2\right)}. \tag{9}$$

This shows that to maintain constant output power, Q_{int} determined by the internal losses (absorption and scattering mostly) must increase as to allow $|r_{2s}|^2$ to approach unity. If these two laser parameters, Q_{int} and r_{2s}, increase in concert, we can then simultaneously reduce the feedback sensitivity of the laser without sacrificing the output power of the laser.

Figure 2(d) graphically illustrates the consequences of the Q-factor of the laser (Q_{int}) on the effective isolation of the laser. For a laser with $Q_{\text{int}} = 1\times10^6$, as is the case on our platform discussed below, a laser can theoretically achieve an effective optical isolation equivalent to 35 dB of isolation compared to an all III-V semiconductor laser which typically has Q_{int} limited to values of $\approx 1\times10^4$ due to material absorption in the doped p- and n-regions. This 35 dB yields the equivalent isolation of a single-stage isolator. In many applications where a single isolator is necessary, such a laser is expected to be able to operate *without any isolator* obviating the need for the magneto-optic material in the photonic platform. Accordingly, every increase by a factor of 2 in the Q-factor of the resonator results in an increase of 6 dB in the effective isolation of the laser emphasizing the potential for this technique to continue to improve the performance of semiconductor lasers, as the losses in semiconductors continue to decrease. Should the intrinsic Q-factor of the resonator be increased to 1×10^7 [23], the laser could achieve an effective isolation upward of 50 dB compared to that of a conventional III-V semiconductor laser.

3. High-*Q* heterogeneous Si/III-V lasers demonstration

To achieve high Q_{int} values, which is the prerequisite to feedback insensitivity, we adopt a resonator design wherein the great majority of the optical energy, up to ~ 99% in our case, resides in the low-loss Si guiding layer (effective index $n_{\text{eff}} \approx 3.3$) rather than in the highly-doped, and thus high-loss III-V layers ($n_{\text{eff}} \approx 3.1$). In these lasers, the total internal Q-factor is given by the combination of the losses in each of the two materials, the low-loss Si, and the high-loss but gain-providing III-V material [6]. This can be summarized by the following equation,

$$\frac{1}{Q_{\text{int}}} = \frac{1-\Gamma_{\text{III-V}}}{Q_{\text{Si}}} + \frac{\Gamma_{\text{III-V}}}{Q_{\text{III-V}}}, \tag{10}$$

where Q_{Si} is an effective Q-factor accounting for the intrinsic and scattering losses in the low-loss Si material, $Q_{\text{III-V}}$ is an equivalent Q-factor accounting for the average loss in the high-loss gain-providing III-V material (often limited by the free-carrier absorption in the material), and $\Gamma_{\text{III-V}}$ is the optical confinement factor in the high-loss III-V material.

An illustration of the structure, using Si as the low-loss material and InGaAsP quantum wells as the gain-providing material, is shown in Figs. 2(a) and (b). In the limit that $\Gamma_{\text{III-V}}$ remains small ($\Gamma_{\text{III-V}} \ll 1$) and as long as the losses in the Si are lower than the losses in the III-V ($Q_{\text{Si}}^{-1} \ll \Gamma_{\text{III-V}} Q_{\text{III-V}}^{-1}$), a condition satisfied over orders of magnitude of $\Gamma_{\text{III-V}}$, Eq. (10) can be approximated to [6],

$$Q_{\text{int}} = \frac{Q_{\text{III-V}}}{\Gamma_{\text{III-V}}(t_{\text{ox}})}. \tag{11}$$

The equation above introduces an important parameter $\Gamma_{\text{III-V}}$ that controls the Q-factor of the resonator, and thus the feedback insensitivity. In our case, the degree of $\Gamma_{\text{III-V}}$ can be controlled by choosing the thickness (t_{ox}) of the silicon dioxide (SiO_2) 'spacer' layer, as shown in Figs. 2(a) and (b). The thicker the thickness of the spacer layer, the smaller the fraction of the energy

Optics EXPRESS

which is stored in the lossy III-V layers, thus leading to higher Q_{int} [6,7,24]. Hence, the intrinsic loss, dominated by free-carrier absorption in III-V layers, is largely reduced. This dramatic increase of Q_{int} allows $|r_{2s}|^2$ to approach unity as discussed above, making the lasers more insensitive to optical feedback. The SiO_2 spacer layer was first introduced in [6,7] as a means to dramatically decrease spontaneous emission into the lasing mode for a monolithically integrated semiconductor laser. Here, we highlight the dual role that this layer takes in controlling the sensitivity to optical feedback of the laser by the virtue that it increases its cold cavity Q-factor. The relatively thick SiO_2 between the Si and III-V acts as a *lever* controlling the lasing mode's intrinsic losses and thus the sensitivity of the laser to optical feedback.

With this insight, we design lasers with the SiO_2 spacer layer thickness 50 nm and 90 nm, corresponding to $\Gamma_{\text{III-V}} = 10\%$ and 3%, respectively (Fig. 2(b)). We estimate $Q_{\text{int}} \approx 1 \times 10^5$ for the 50 nm and $Q_{\text{int}} \approx 3 \times 10^5$ for the 90 nm spacer laser, respectively. The strategy continues to increase the intrinsic Q-factor of the laser until the losses from the III-V ($Q_{\text{III-V}}/\Gamma_{\text{III-V}}$) become comparable to the intrinsic losses in the Si resonator (Q_{Si}), in our case, limited to $Q_{\text{Si}} \approx 1 \times 10^6$. If one attempts to further reduce the confinement factor in the III-V, and correspondingly in the gain-providing QWs, this results in an increase in the threshold carrier density required to achieve threshold because the losses in the cavity become limited by the losses in the Si. For our structure, we estimate the limit $Q_{\text{Si}} \approx Q_{\text{III-V}}/\Gamma_{\text{III-V}}$ to occur when the spacer thickness is approximately 150 nm [6]. Our finite element simulations in Comsol Multiphysics estimate that for lasers with the 150 nm spacer, $\Gamma_{\text{III-V}} = 1\%$ and $\Gamma_{\text{Si}} = 99\%$. The expected effective isolation for each of the quoted SiO_2 thicknesses is summarized in Fig. 2(d). The 50 nm and 90 nm spacer lasers are expected to yield more than 20 dB and 27 dB of optical isolation compared to an all III-V semiconductor laser. If the fabrication losses and absorption losses in the Si material could be decreased, one may then continue to increase the thickness of the oxide layer beyond the stated 150 nm to achieve even larger resonator Q, and even larger feedback insensitivity.

The high-Q resonator is formed in a Si waveguide patterned with a 1D grating as shown in Fig. 2(c), and the fabrication procedure is outlined in [6,7,24]. The rib waveguide has a width of 2.5 μm and an etch depth of 60 nm in the Si device layer chosen to minimize sidewall scattering losses. The grating is designed with a constant period ($\Lambda = 240$ nm) and width in the transverse direction ($W_z = 120$ nm) which determine the resonant wavelength. The width of the grating varies over a length of 120 μm from a width of $W_x = 300$ nm to a maximum value of $W_x = 515$ nm at the center of the grating. A 240 μm defect regime is surrounded by two mirror regions on either side, 300 μm and 400 μm long for the 50 nm and 90 nm spacer laser respectively, that provide the necessary reflections for the resonator. The dimensions of the grating in the mirror sections are $W_z = 120$ nm and $W_x = 300$ nm. The mirror length of the 90 nm spacer laser is chosen to be larger than that of the 50 nm spacer laser to increase the loaded Q-factor of the 90 nm spacer laser proportionally to the expected increase in the intrinsic Q-factor.

4. Measurement of the feedback sensitivity of the lasers

To estimate the sensitivity of the fabricated lasers to optical feedback, we quantify the reflectivity of an external reflector (R_{ext}) at which the transition into the coherence collapse regime occurs. Coherence collapse will manifest itself as (1) a dramatic increase in the linewidth of the laser [25–27] and (2) a near total disappearance of the fringe visibility (β) of the interference in the output signal. In our experiments, we use a Mach-Zehnder interferometer (MZI) with a free spectral range (FSR) of 533 MHz and define the transition to the coherence collapse regime as the point where the fringe visibility is reduced to 70% of its maximum value of 1. The fringe visibility is quantified as the ratio between the amplitude of the interference term and the DC term as measured on a photodetector as the path length mismatch of the interferometer is changed

Optics EXPRESS

by a few wavelengths

$$\beta = \frac{V_{\max} - V_{\min}}{V_{\max} + V_{\min}}, \tag{12}$$

where $V_{\max}$ and $V_{\min}$ are the maximum and minimum voltage measured on a photodetector collecting light from the interferometer as shown in Fig. 3. The output of the laser is divided into two separate paths, a feedback path in polarization-maintaining fiber, and a characterization path in single-mode fiber. In the feedback path, a booster optical amplifier (Thorlabs BOA1004P), followed by a variable attenuator is used to control the output power fraction fed back into the laser. Calibrated power taps are used to estimate the laser output and reflected power in the lensed fiber, and the external reflectivity is estimated as $R_{\text{ext}} = \eta_{\text{f}}^2 P_{\text{reflected}}/P_{\text{out}}$, where η_{f} is the coupling efficiency into single-mode fiber. The amplifier is used to overcome the finite coupling efficiency of light into single-mode fiber (typically in the range of $20-40\%$ for our system) as well as the finite insertion loss in the couplers and attenuator used (measured to be $1-2$ dB per component) enabling the measurement of the fringe visibility near reflectivities approaching 100%. As the reflectivity is increased, the onset of coherence collapse is determined by measuring the fringe visibility of the voltage measured on the photodetector (V_{PD}) as the phase condition of the interferometer ($\frac{2\pi}{\lambda/n}\Delta L$) is changed

$$V_{\text{PD}}(\Delta L) = V_0\left(1 + \beta \sin\left(\frac{2\pi}{\lambda/n}L + \frac{2\pi}{\lambda/n}\Delta L\right)\right), \tag{13}$$

where L is the nominal path length mismatch of the interferometer, n is the refractive index of fiber, λ is the wavelength of the laser, and ΔL is the change in the path length of the MZI as the piezo-electric motor changes the path length of the interferometer by a few wavelengths at an actuation frequency of 1 kHz. The fringe visibility is related to the FSR of the MZI and the linewidth of the laser ($\Delta\nu$) by [21]

$$\beta = e^{-\Delta\nu/\text{FSR}}. \tag{14}$$

The fringe visibility of the interferometer will drop rapidly once the linewidth of the laser under the external feedback becomes comparable or larger to the FSR of the interferometer. In all measurements, the fringe visibility is measured 10 times for a given value of the external reflector.

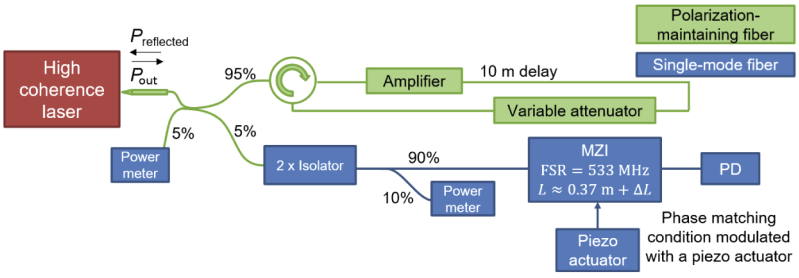

Fig. 3. The experimental setup used to measure the onset of coherence collapse. The fringe visibility of the MZI is characterized as the magnitude of the reflection is increased. The magnitude of the reflection is controlled by a variable attenuator and a booster optical amplifier placed inline in polarization-maintaining fiber to ensure that the reflection is in the same polarization as the lasing mode. The amplifier is used to enable R_{ext} to approach unity while accounting for the losses in coupling to fiber and in various passive components.

Figure 4(a) shows the output power as a function of current for the 50 nm and 90 nm spacer heterogeneous Si/III-V lasers. Also included is a comparison to a commercial all III-V DFB

Optics EXPRESS

laser representative of lasers employed in communication systems (a fiber pigtailed Mistubishi ML9XX InGaAsP DFB with a linewidth of approximately 1 MHz). The optical path length of the reflector was 10 m in fiber. Figure 4(b) shows an example of the progression of the fringe visibility as the reflection is increased for the 90 nm spacer laser. The fringes remain visible for the laser even at the external reflectivity of 0.3 dB in contrast to the case of the 50 nm spacer laser where they become invisible at an external reflectivity of -7.1 dB. Figure 4(c) shows the fringe visibility as a function of the external reflectivity for all the lasers operating at a bias current of 2× threshold.The 50 nm spacer laser maintains its high coherence properties up to an external reflectivity of −20 dB while the 90 nm spacer laser maintains a fringe visibility near unity up to a reflectivity of −15 dB. The 90 nm spacer laser, due to employing mirrors with higher reflectivity, is less sensitive to optical feedback than the 50 nm spacer laser. For comparison, the commercial all III-V DFB laser exhibits signs of instability near −50 dB and reaches coherence collapse (where the fringe visibility begins to oscillate) at a reflectivity of −40 dB. Thus, the high-Q Si/III-V lasers have an equivalent isolation of *20 dB* for the case of the 50 nm spacer and *25 dB* for the case with the 90 nm spacer relative to conventional all III-V DFB lasers. A slight increase in the value of Q_{int}, now in the works, should obviate the need for optical isolators altogether. The work in [28] expands on these experiments to demonstrate the same technology used in an optical communication setting where the high-Q spacer laser is able to operate with the low optical signal to noise penalty under the presence of external feedback.

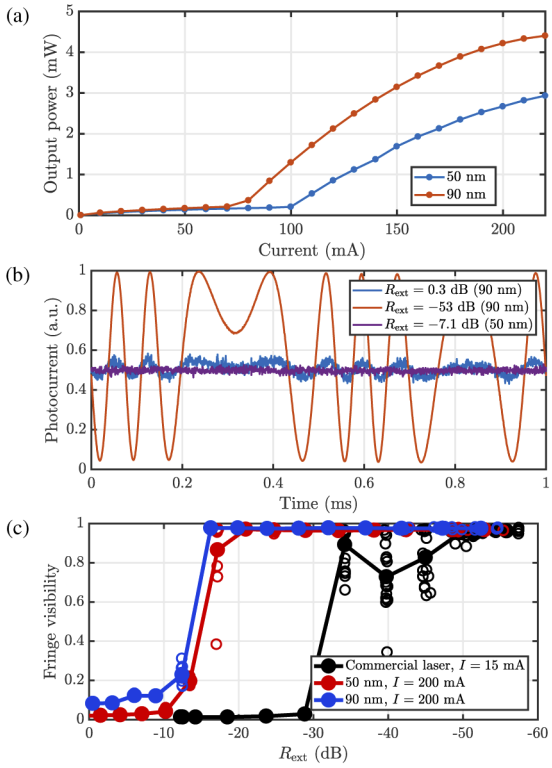

Fig. 4. (a) The light-current characteristics of the high-Q heterogeneous Si/III-V lasers with the 50 nm and 90 nm spacer that were tested for their feedback sensitivity. (b) The raw data obtained from the fringe visibility experiment of the lasers. (c) The fringe visibility as a function of the external reflectivity for the two lasers compared to the commercial all III-V DFB laser. The measurements shown in (b) and (c) are taken at bias currents of 200 mA for the 50 nm and 160 mA for the 90 nm spacer laser.

Optics EXPRESS

For completeness, Fig. 5 shows measurements of the optical spectrum of the lasers as measured from an optical spectrum analyzer (OSA) under the presence of optical feedback. Since the linewidth of the laser is consistently less than the resolution of the OSA, the traces with, and without optical feedback are nearly identical. However, this measurement confirms that no competing optical side-bands are present in the spectrum ensuring the compatibility of this strategy with optical frequency multiplexing.

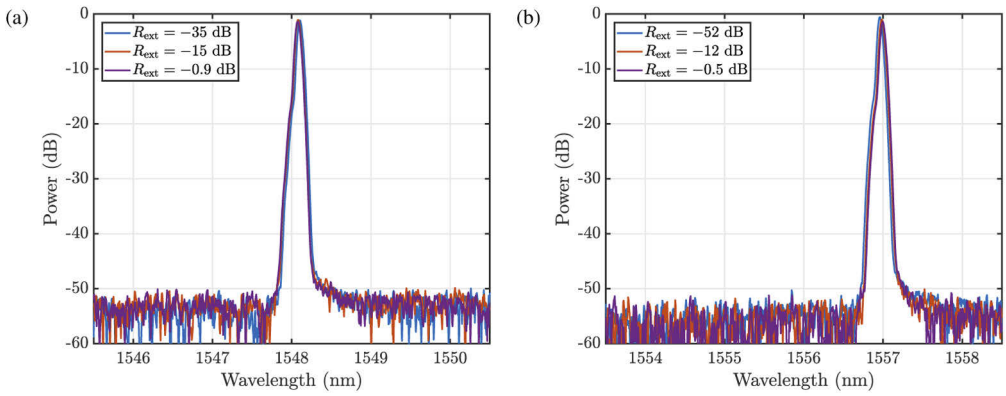

Fig. 5. The optical spectrum of the high-Q heterogeneous Si/III-V laser with (a) the 50 nm and (b) the 90 nm spacer as measured with an optical spectrum analyzer under various levels of optical feedback.

5. Conclusions

We demonstrated that heterogeneous Si/III-V lasers with intrinsic, i.e. not external, very high-Q resonators are immune to coherence collapse in the presence of as high as −15 dB external reflections. This represents an effective isolation of *up to 25 dB* compared to typical commercial all III-V DFB lasers. By taking advantage of the low intrinsic losses in Si, the external Q-factor is increased by utilizing higher reflectivity mirrors thereby diminishing the effect of optical feedback on the circulating field. The employment of materials with lower losses than Si in the future would lead to even larger feedback insensitivity. These lasers would have isolation characteristics comparable to the current state of the art III-V lasers with greater than 35 dB isolators with only modest increases in the resonator intrinsic-Q paving the way for isolator-free integrated photonics.

Funding

Defense Advanced Research Projects Agency (N66001-14-1-4062); Army Research Office (W911NF-14-P- 0020, W911NF-15-1-0584, W911NF-16-C-0026).

Disclosures

The authors declare no conflicts of interest.

References

1. C. T. Santis, S. T. Steger, Y. Vilenchik, A. Vasilyev, and A. Yariv, "High-coherence semiconductor lasers based on integral high-Q resonators in hybrid Si/III-V platforms," Proc. Natl. Acad. Sci. **111**(8), 2879–2884 (2014).
2. M. J. R. Heck, J. F. Bauters, M. L. Davenport, J. K. Doylend, S. Jain, G. Kurczveil, S. Srinivasan, Y. Tang, and J. E. Bowers, "Hybrid silicon photonic integrated circuit technology," IEEE J. Sel. Top. Quantum Electron. **19**(4), 6100117 (2013).

Optics EXPRESS

3. K. Aiki, M. Nakamura, J. Umeda, A. Yariv, A. Katzir, and H. W. Yen, "GaAs "GaAlAs distributed" feedback diode lasers with separate optical and carrier confinement," Appl. Phys. Lett. **27**(3), 145–146 (1975).
4. M. Nakamura, K. Aiki, J. Umeda, and A. Yariv, "cw operation of distributed "feedback GaAs" GaAlAs diode lasers at temperatures up to 300 K," Appl. Phys. Lett. **27**(7), 403–405 (1975).
5. M. Nakamura, K. Aiki, J. Umeda, A. Yariv, H. W. Yen, and T. Morikawa, "GaAs-$Ga_{1-x}Al_xAs$ double-heterostructure distributed-feedback diode lasers," Appl. Phys. Lett. **25**(9), 487–488 (1974).
6. C. T. Santis, Y. Vilenchik, N. Satyan, G. Rakuljic, and A. Yariv, "Quantum control of phase fluctuations in semiconductor lasers," Proc. Natl. Acad. Sci. **115**(34), E7896–E7904 (2018).
7. C. T. Santis, Y. Vilenchik, A. Yariv, N. Satyan, and G. Rakuljic, "Sub-kHz quantum linewidth semiconductor laser on silicon chip," in *CLEO: 2015 Postdeadline Paper Digest* (Optical Society of America, 2015), p. JTh5A.7.
8. K. Petermann, *Laser Diode Modulation and Noise* (Springer, Netherlands, Dordrecht, 1988).
9. J. Helms and K. Petermann, "Microwave modulation of laser diodes with optical feedback," J. Lightwave Technol. **9**(4), 468–476 (1991).
10. K. Petermann, "External optical feedback phenomena in semiconductor lasers," IEEE J. Sel. Top. Quantum Electron. **1**(2), 480–489 (1995).
11. C. Henry, "Theory of the linewidth of semiconductor lasers," IEEE J. Quantum Electron. **18**(2), 259–264 (1982).
12. K. Vahala, L. C. Chiu, S. Margalit, and A. Yariv, "On the linewidth enhancement factor α in semiconductor injection lasers," Appl. Phys. Lett. **42**(8), 631–633 (1983).
13. N. Schunk and K. Petermann, "Numerical analysis of the feedback regimes for a single-mode semiconductor laser with external feedback," IEEE J. Quantum Electron. **24**(7), 1242–1247 (1988).
14. J. Helms and K. Petermann, "A simple analytic expression for the stable operation range of laser diodes with optical feedback," IEEE J. Quantum Electron. **26**(5), 833–836 (1990).
15. J. Helms and K. Petermann, "Microwave modulation of laser diodes with optical feedback," J. Lightwave Technol. **9**(4), 468–476 (1991).
16. J. Wang, H. Hu, H. Yin, Y. Bai, J. Li, X. Wei, Y. Liu, Y. Huang, X. Ren, and H. Liu, "1.3 μm InAs/GaAs quantum dot lasers on silicon with GaInP upper cladding layers," Photonics Res. **6**(4), 321–325 (2018).
17. H. Huang, J. Duan, B. Dong, J. Norman, D. Jung, J. E. Bowers, and F. Grillot, "Epitaxial quantum dot lasers on silicon with high thermal stability and strong resistance to optical feedback," APL Photonics **5**(1), 016103 (2020).
18. A. Y. Liu, T. Komljenovic, M. L. Davenport, A. C. Gossard, and J. E. Bowers, "Reflection sensitivity of 1.3 μm quantum dot lasers epitaxially grown on silicon," Opt. Express **25**(9), 9535–9543 (2017).
19. H. Huang, J. Duan, B. Dong, J. Norman, D. Jung, J. E. Bowers, and F. Grillot, "Epitaxial quantum dot lasers on silicon with high thermal stability and strong resistance to optical feedback," APL Photonics **5**(1), 016103 (2020).
20. A. Yariv, *Quantum Electronics* (Wiley, 1967).
21. A. Yariv and P. Yeh, *Photonics - Optical Electronics in Modern Communications*, 6th ed (Oxford, 2007).
22. S. Steger, *A fundamental approach to phase noise reduction in hybrid Si/III-V lasers* (California Institute of Technology, 2014).
23. T. Asano, Y. Ochi, Y. Takahashi, K. Kishimoto, and S. Noda, "Photonic crystal nanocavity with a Q factor exceeding eleven million," Opt. Express **25**(3), 1769–1777 (2017).
24. H. Wang, D. Kim, M. Harfouche, C. T. Santis, N. Satyan, G. Rakuljic, and A. Yariv, "Narrow-linewidth oxide-confined heterogeneously integrated Si/III-V semiconductor lasers," IEEE Photonics Technol. Lett. **29**(24), 2199–2202 (2017).
25. D. Lenstra, B. Verbeek, and A. Den Boef, "Coherence collapse in single-mode semiconductor lasers due to optical feedback," IEEE J. Quantum Electron. **21**(6), 674–679 (1985).
26. F. Grillot, B. Thedrez, and G.-H. Duan, "Feedback sensitivity and coherence collapse threshold of semiconductor DFB lasers with complex structures," IEEE J. Quantum Electron. **40**(3), 231–240 (2004).
27. R. Tkach and A. Chraplyvy, "Regimes of feedback effects in 1.5 μ m distributed feedback lasers," J. Lightwave Technol. **4**(11), 1655–1661 (1986).
28. Z. Zhang, K. Zou, H. Wang, P. Liao, N. Satyan, G. Rakuljic, A. E. Willner, and A. Yariv, "High-speed coherent optical communication with isolator-free heterogeneous Si/III-V lasers," J. Lightwave Technol. **38**(23), 6584–6590 (2020).